

PRELIMINARY CHARACTERISTIC OF ELECTRICAL NON-LINEARITY CO DOPED CMO-ZNO BASED VARISTOR CERAMIC

Article history

Received

15 August 2015

Received in revised form

15 November 2015

Accepted

30 December 2015

Muhamad Azman Zulkifli^{a*}, Mohd Sabri Mohd Ghazali^a, Wan Rafizah Wan Abdullah^b, Azmi Zakaria^c, Zakiyah Ahmad^a

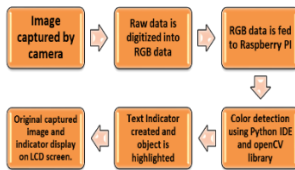
*Corresponding author
gsk2013@pps.umt.edu.my

^aSchool of Fundamental Science, Universiti Malaysia Terengganu, 21030 Kuala Terengganu, Terengganu, Malaysia

^bSchool of Ocean Engineering, Universiti Malaysia Terengganu, 21030 Kuala Terengganu, Terengganu, Malaysia

^cDepartment of Physics, Faculty of Science, Universiti Putra Malaysia, 43400 UPM Serdang, Selangor, Malaysia

Graphical abstract



Abstract

Zinc oxide based varistor are widely used as circuit protective devices by literally absorbs these dangerous surge and spikes or grounding this unwanted magnitudes. In this research, zinc oxide is added with 20 mol% calcium manganite (CaMnO_3) as an additive and Cobalt oxide (CoO) as doping material. Citrate-gel method is used as fabrication method compared to conventional solid-state method. This compound ($\text{ZnO-CaMnO}_3\text{-CoO}$) undergoes pre-sintering at 500°C for 2 hours. In the sintering process, sintering temperature at 1300°C , while the sintering time are setting at 1.5 hours. X-ray diffraction (XRD) patterns shows the components and phases of the compounds. The change of functional group was observed by Furrier transform infra-red (FTIR). I-V characteristic shows the value of nonlinear coefficient in the range of 1.0-2.0.

Keywords: Zinc oxide, varistor; citrate-gel

Abstrak

Varistor berasaskan zink oksida digunakan secara meluas sebagai litar peranti perlindungan yang berperanan menyerap lonjakan berbahaya dan pancang atau pembumian magnitud yang tidak diinginkan. Dalam kajian ini, zink oksida ditambah dengan 20 % mol CaMnO_3 sebagai bahan tambahan dan oksida kobalt sebagai bahan dop. Kaedah Citrate-gel digunakan sebagai kaedah fabrikasi berbanding kaedah keadaan pepejal konvensional. Kompaun ini ($\text{ZnO - CaMnO}_3\text{-CoO}$) mengalami pra- pensinteran pada 500°C selama 2 jam. Dalam proses pensinteran, suhu pensinteran ditetapkan pada 1300°C , manakala masa pensinteran ditetapkan selama 1.5 jam. Keputusan pembelauan sinar-X (XRD) menunjukkan komponen dan fasa yang terdapat dalam sebatian. Perubahan kumpulan berfungsi diperhatikan menggunakan *Furrier transform infra-red (FTIR)*. Pengujian IV menunjukkan nilai pekali linear di dalam julat 1.0-2.0.

Kata kunci: Zinc oksida, varistor; citrate-gel

© 2016 Penerbit UTM Press. All rights reserved

1.0 INTRODUCTION

Wildly used of ZnO in multiple field research area make it become as promising semiconductor material

especially in solar cells [1, 2], UV laser, chemical and biological sensor, photocatalyst [3] and so do varistor [4-6]. ZnO is an important and well as n-type semiconductor with a wide direct band gap (3.37 eV)

and large excitation binding energy (60 meV). Specialty possessing high nonlinear properties of current voltage characteristic make ZnO extensively use as surge protectors in power systems and electronic circuit. This ZnO based varistor literally absorb the transient voltage [7, 8].

Up to date, the varistor research are focusing in producing the low voltage varistor. Introduce calcium manganite (CaMnO) as additive material has been reported by [9]. Intensive study of additive CaMnO to produce low voltage varistor by [9, 10] shows a significant result. Beside the CaMnO₃, praseodymium oxide (PrO) also shows a potential doping material in order to produced low voltage varistor [11-13].

In the other hand, doping elements of rare-earth also shows a potential to be used as doping low voltage varistor [14]. Effect doping of Erbium (Er), lanthanum (La) and Cobalt (Co) also reported as suitable doping material in varistor ceramics application.

In this work, the combination of CaMnO₃ as additive and Co as doping material in ZnO based varistor ceramics is investigate. As a first step on revealed the potential of this combination, a preliminary study of electrical non-linearity are performed. This varistor ceramic are synthesis by sol-gel method and characterize by XRD, FTIR and IV source measure unit.

2.0 EXPERIMENTAL

2.1 Materials

Raw materials were prepared according to the composition of 78.5 mol % ZnO + 20.0 mol % CaMnO₃ + 1.5 mol % CoO. Reagent Calcium acetate monohydrate with the purity of 99.0% (Sigma Aldrich), Manganese (II) acetate – 4 – hydrate (Hamburg Chemical) and Cobalt (II) acetate (Fisher Chemicals) was used as metal salt precursor and citric acid anhydrous (C₂H₆O₈) with the purity of 99.5% (Alfa Aesar) was selected as the complexing agent. ZnO powder with the particle size of less than 1 μm and 99.9% purity (Sigma Aldrich) was selected as the host material.

2.2 Samples Preparation

Fully coating of Ca-Mn-Co citrate gel with ZnO particles was produced by adding ZnO powder into bath solution that comprising Ca-Mn-Co acetate and citric acid in medium of deionized water. This gel moisture were continues stir for 1 hour retention time at 60 to 80 °C. The molar ratio of calcium acetate/ manganese (II) acetate/ cobalt(II) acetate to citric acid anhydrous was fixed at 1:2 and vigorous stirring was applied to improve the contact.

Uniform coating of Ca-Mn-Co citrate gel with ZnO particles was produced by immersing ZnO powder in bath solution containing citric acid and Ca-Mn-Co acetate in deionized water medium for 1 hour retention time at 70–80 °C. Then, this mixtures dried at

120 °C for 19 h to produce powder with particle size of less than 100 μm. The dried powder was then calcined at 500 °C for 4 h at heating rate of 3 °C/min. The calcined powder comprising 1.75 wt.% polyvinyl alcohol binder was pressed into pellets with 13.0 mm diameter and 1.3 mm thickness using Specac Hydraulic Press machine. The pellet was finally sintered at 1300 °C for 1.5 h in a box furnace (CMTS Model HTS 1400).

2.3 Characterizations

2.3.1 XRD

The phase structure of ZnO-CaMnO₃-CoO compounds before and after sintering were measured using Rigaku Mini Flex II Diffractometer with Cu K_α radiation. A small amount sample (compound sample) was spread uniformly on the sample holder, 2θ scan were carried out over the diffraction angles from 5° to 80° at the speed of 2.00°/min.

2.3.2 FTIR

Functional group of compound elements in stage after calcined and after sintering were identified using IRTracer-100 Fourier Transform Infrared Spectrophotometer (SHIMADZU). 1:7 ratio were mixed and prepared between samples compound to KBr. The compressed transparence film (sample compound) exposed to infrared penetration starting wavelength of 400 cm⁻¹ until the stop wavelength at 4000 cm⁻¹.

2.3.3 I-V Source Measure Unit

Electrical behavior of pelleted sintered sample were measured using a KEITHLEY 4200-SCS Semiconductor Characterization System. 15Wt% and pure silver conductive paint were place on the both side of samples as an electrodes. The nonlinear coefficient (α) was determined from the equation (1),

$$\alpha = \frac{dI/I}{dV/V} = \frac{d(\log I)}{d(\log V)} \approx \frac{\log_{10} I_2 - \log_{10} I_1}{\log_{10} V_2 - \log_{10} V_1} \quad (1)$$

3.0 RESULTS AND DISCUSSION

3.1 XRD

XRD patterns of pure ZnO before and after sintering are shown in Figure 1.

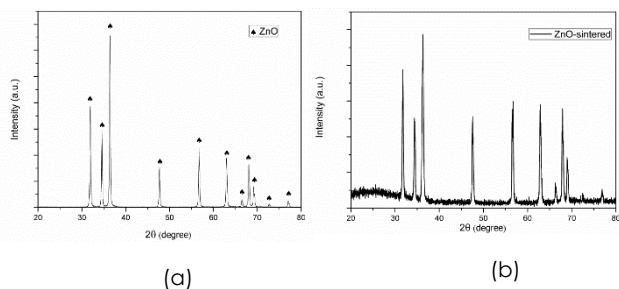


Figure 1 (a) Starting powder ZnO. (b) ZnO after sintered

Figure 1 (a) and (b) shows all diffraction peaks in a good agreement with single phase polycrystalline hexagonal ZnO of wurtzite structure according to ICSD code: 067454 [15]. The scattered plot of Figure 1(b) indicated the change of crystallite size or grain size of ZnO after undergoes sintering process at 1300 °C. The formation of CaMnO_3 in the sintered compound ZnO-CaMnO_3 observed by the presence of minor peaks as shown in Figure 2.

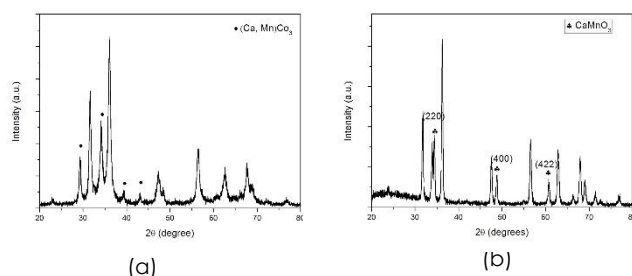


Figure 2 (a) $\text{ZnO-CaMnO}_3\text{-CoO}$ after calcined. (b) $\text{ZnO-CaMnO}_3\text{-CoO}$ after sintered

Figure 2 (a) shows the appeared of manganocalcite ($(\text{Ca, Mn})\text{CO}_3$) peaks. Appeared peaks identified using Crystallographica Search-match and its shows the good match with reference Pdf No: 2-604 and Pdf N0: 2-630. However, after sintered process disappeared of $(\text{Ca, Mn})\text{CO}_3$ peaks suggest carbonate (CO_3) compound released during the sintering process. Throughout the sintering process, $(\text{Ca, Mn})\text{CO}_3$ expected transform to CaMnO_3 . Transformation result indicated by the appearing minor peaks of CaMnO_3 in Figure 2 (b). Figure 2 (b) shows the reveals of hkl plane in perovskite structures CaMnO_3 at 34° (2,2,0), 49° (4,0,0) and 61° (4,2,2) shows the good agreements with [16] and [17].

Beside the transformation process, Figure 2 (b) also shows the ZnO-CaMnO_3 become highly crystalline. Its obviously can see by decreasing of peaks broadening. The differ peaks broadening illustrated the change of inhomogeneous crystallize size and also microstrain in the compound.

Same phenomena occur in $\text{ZnO-CaMnO}_3\text{-CoO}$ compound between before and after sintered process. Figure 3 shows the XRD result in stages of before and after sintering at 1300°C.

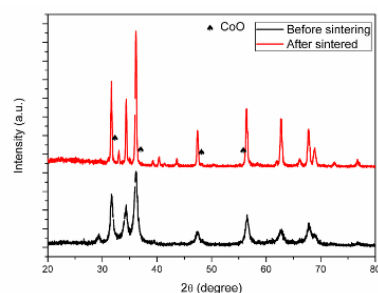


Figure 3 $\text{ZnO-CaMnO}_3\text{-CoO}$ before and after sintered

Identification of CoO peaks are referring to Pdf No: 89.2803 and Pdf No: 75.419. No additional reflections by the CoO were observed in Figure 3 [18]. This result suggests that the dopant is well substituted in the ZnO lattice and the wurtzite structure is not tailored by the addition of Co into the ZnO matrix at least up to the detection level of XRD [19]. This behaviour is possible due to the small difference in radii between divalent, high-spin Co in tetrahedral coordination (0.58 \AA) and divalent Zn in tetrahedral coordination (0.60 \AA) [20-22]

3.2 FTIR

FTIR analysis in Figure 4 shows the complexation of ZnO-CaMnO_3 compound before sintering, while $\text{ZnO-CaMnO}_3\text{-CoO}$ compound before and after sintered.

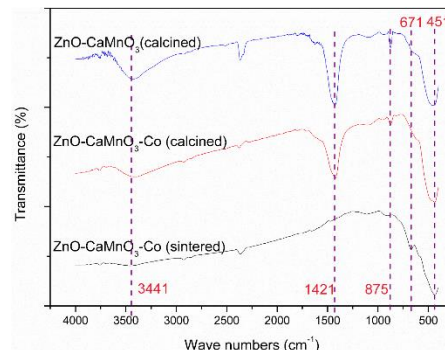


Figure 4 FTIR analysis of compounds

It was found that non sintered compound contained ZnO and Ca, Mn, Co complexes. In phase pure ZnO very intense peak are observed in wavenumber range of 600 cm^{-1} to 400 cm^{-1} . This intense peak also reported by [23-27] in their works. Besides the ZnO bonding, CoO bond also indicated by the appearance week peak at 671 cm^{-1} [28]

The loss of several characteristic peaks in region of $600\text{-}2500 \text{ cm}^{-1}$ in calcined compound, were associated to removing of carbonyl (C=O), carboxylate and alkyl regarding to high temperature during sintering process [11]. The obviously disappearance of peak at 1421 cm^{-1} and peak 875 cm^{-1} , shows the removing of carbonate group ($-\text{CO}_3$)

[11, 28, 29]. Removing of this $-\text{CO}_3$ aligned with the XRD results in this work.

The boarding peaks in range of $2750\text{--}3750\text{ cm}^{-1}$ represents the OH bond with the free ion in $3600\text{--}3650\text{ cm}^{-1}$ and H bonded at $3200\text{--}3500\text{ cm}^{-1}$ [30, 31]. The removing of OH bond are related with change to highly crystalline of ceramic after sintered as shown by XRD results in Figure 2 and Figure 3.

3.3 I-V

Table 1 shows the value of non-linear coefficient (α) for ZnO-CaMnO₃-CoO and ZnO-CaMnO₃ compounds.

Table 1 Comparison of α

compound	Non-linear coefficient (α)	Standard error
ZnO-CaMnO ₃	1.3530	0.00237
ZnO-CaMnO ₃ -CoO	1.6212	0.00256

Additive of CaMnO₃ on the compound system shown obviously change regarding to breakdown voltage of this varistor. This CaMnO₃ shows a good agreement with the [9] in order to produces low voltage varistor. The value of α slightly increase by the effect of small doping Co into the samples [32].

4.0 CONCLUSION

Structure and complexation of both ceramics and its precursor powder were examined by XRD shows the change in crystallite size through decreasing of peaks broadening, change of inhomogeneous crystallite size and also microstrain in the compound are suggested occurs. FTIR analysis confirmed the chemical changes during citrate gel reaction and elimination of organic functional groups during calcination or sintering to produce dense ZnO-CaMnO₃-CoO ceramics. The nonlinear coefficient (α) ZnO-CaMnO₃-CoO ceramics as a function of sintering time was monitored using I-V characteristic measurement. The α value increased proportionally with the doping of Co contents. The value slightly increased in the range of 1.0-2.0.

Acknowledgement

The authors would like to express gratitude and acknowledgement to Ministry of Higher Education Malaysia for funding this project under Research University Grant Scheme (RUGS) of Project No. 05-01-09-0754RU.

References

- [1] Belaidi, A., Dittrich, T., Kieven, D., Tornow, J., SchwarzburgK. and Lux-Steiner, M. 2008. Influence Of The Local Absorber Layer Thickness On The Performance Of ZnO Nanorod Solar Cells. *Physica Status Solidi (RRL)-Rapid Research Letters*. 2(4): 172-174.
- [2] Katayama, J., Ito, K., Matsuoka, M. and Tamaki, J. 2004. Performance of Cu₂O/ZnO Solar Cell Prepared By Two-Step Electrodeposition. *Journal of Applied Electrochemistry*. 34(7): 687-692.
- [3] Zhang, X., Qin, J., Xue, Y., Yu, P., Zhang, B., Wang, L., Liu, R. 2014. Effect Of Aspect Ratio And Surface Defects On The Photocatalytic Activity Of ZnO Nanorods. *Scientific Reports*. 4.
- [4] Sabri, M., Azmi, B., Rizwan, Z., Halimah, M., Hashim, M., Zaid, M. 2011. Effect Of Temperature Treatment On The Optical Characterization Of ZnO-Bi₂O₃-TiO₂ Varistor Ceramics. *International Journal of Physical Sciences*. 6(6): 1388-1394.
- [5] Rizwan, Z., Zakaria, A., Ghazali, M. S. M. 2011. Photopyroelectric Spectroscopic Studies Of ZnO-MnO₂-Co₃O₄-V₂O₅ Ceramics. *International Journal Of Molecular Sciences*. 12(3): 1625-1632.
- [6] Rizwan, Z., Sabri, M. and Azmi, B. 2011. Photopyroelectric Characteristics Of Pr₆O₁₁-ZnO Ceramic Composites. *International Journal of Physical Sciences*. 6(1): 79-83.
- [7] Drabkin, M. 2002. Surge Protection Of Low-Voltage AC Power By MOV-Based SPDs. *Harmonics and Quality of Power, 10th International Conference*. IEEE.
- [8] Eilers, K. W., Wingate, M. and Pham, E. 2000. Application And Safety Issues For Transient Voltage Surge Suppressors. *Industry Applications, IEEE Transactions*. 36(6): 1734-1740.
- [9] Vijayanandhini, K. and Kuttly, T.R.N. 2006. Low-Voltage Varistors From Zn O + CaMnO₃ Ceramics. *Applied Physics Letters*. 88(123513).
- [10] Vijayanandhini, K., Kuttly, T. 2007. Calcium Zinc Manganites, Ca₄ Mn₇ Zn₃ O₂₁₋₆ (0.5 < δ < 2.5) With Beta-Alumina Or Magnetoplumbite-Type Structure And Their Nonlinear Electrical Transport And Magnetic Properties. *Materials Letters*. 61(17): 3652-3657.
- [11] Abdullah, W. R. W., Zakaria, A. Ghazali, M.S.M. 2012. Synthesis Mechanism Of Low-Voltage Praseodymium Oxide Doped Zinc Oxide Varistor Ceramics Prepared Through Modified Citrate Gel Coating. *International Journal of Molecular Sciences*. 13(4): 5278-5289.
- [12] Nahm, C. W. 2011. Pulse Aging Behavior of ZnO-Pr₆O₁₁-CoO-Cr₂O₃-Dy₂O₃ Varistor Ceramics With Sintering Time. *Ceramics Internationa*. 137: 1409-1414.
- [13] Nahm, C. W. 2014. Microstructure And Varistor Properties Of Y₂O₃-doped ZnO-Pr₆O₁₁-CoO-Cr₂O₃-La₂O₃ ceramics. *Ceramics International*. 40(1,B): 2477-2481.
- [14] Jiang, F., Peng, Z., Zang, Y., Fu, X. 2013. Progress On Rare-Earth Doped ZnO-Based Varistor Materials. *J Adv Ceram*. 2(3): 201-212.
- [15] Ghazali, M. S. M., Zakaria, A., Abdullah, W. A. W., Zaid, M. A. M., Matori, K. A. 2015. Effect of Co₃O₄ Doping on Nonlinear Coefficient in Zn-Bi-Ti-O Varistor Ceramics. *Advanced Materials Research*. 1107: 20-26.
- [16] Kafash, S., Moghadam, T. G., Kompany, A., S.M. Hosseini, S. M. 2014. Structural and Electrical Properties of CaMnO₃ Prepared Via Sol-gel and Solid State Reaction Techniques. *Conference on Nanoscience and Nanotechnology*.
- [17] Kompany, A. 2011. Relaxation Behavior of Néel Temperature in Micro and Nanosized Particles of CaMnO₃. *The International Conference for Nanomaterials Synthesis and Characterization (INSC 2011)*.
- [18] Freedman, J. J., Kennedy, L. J., Kumar, R. T., Sekaran, G. and Vijaya, J. J. 2010. Studies On The Structural And Optical Properties Of Zinc Oxide Nanobushes And Co-Doped ZnO Self-Aggregated Nanorods Synthesized By Simple Thermal Decomposition Route. *Materials Research Bulletin*. 45(10): 1481-1486.
- [19] Sharma, P. K., Dutta, R. K. and Pandey, A.C. 2010. Alteration Of Magnetic And Optical Properties Of Ultrafine Dilute

- Magnetic Semiconductor ZnO: Co²⁺ Nanoparticles. *Journal Of Colloid And Interface Science*. 345(2): 149-153.
- [20] Nirmala, M. and Anukaliani, A. 2011. Characterization Of Undoped And Co Doped ZnO Nanoparticles Synthesized By DC Thermal Plasma Method. *Physica B: Condensed Matter*. 406(4): 911-915.
- [21] Shannon, R. T. 1976. Revised Effective Ionic Radii And Systematic Studies Of Interatomic Distances In Halides And Chalcogenides. *Acta Crystallographica Section A: Crystal Physics, Diffraction, Theoretical and General Crystallography*. 32(5): 751-767.
- [22] Lima, M. K., Fernandes, D. M., Silva, M. F., Baesso, M. L., Neto, A. M., Morais, G. R., Nakamura, C. V., Caleare, A. O., Hechenleitner, A. A. W., Pineda, E. A. G. Co-Doped ZnO Nanoparticles Synthesized By An Adapted Sol–Gel Method: Effects on The Structural, Optical, Photocatalytic and Antibacterial Properties. *J Sol-Gel Sci Technology*. 72(2): 301-309.
- [23] Zayat, Marcos Levy, M. and David. 2000. Blue CoAl₂O₄ Particles Prepared by the Sol–Gel and Citrate–Gel Methods. *Chemistry of Materials*. 12(9): 2763-2769.
- [24] Li, H., Wang, J., Liu, H., Yang, C., Xu, H., Li, X., Cui, H. 2004. Sol–Gel Preparation Of Transparent Zinc Oxide films With Highly Preferential Crystal Orientation. *Vacuum*. 77: 57-62.
- [25] Anas, S., Mukundan, P., Sanoj, A. M., Mangalaraja, V. R., Ananthakumar, S. 2010. Synthesis Of ZnO Based Nanopowders Via A Non-Hydrolytic Sol Gel Technique And Their Densification Behaviour And Varistor Properties. *Processing and Application of Ceramics*. 4(1): 7-14.
- [26] Zak, A. K., Abrishami, M. E., Majid, W. H. A., Yousefi, R., Hosseini, S. M. 2011. Effects Of Annealing Temperature On Some Structural And Optical Properties Of ZnO Nanoparticles Prepared By A Modified Sol–Gel Combustion Method. *Ceramics International*. 37: 393-398.
- [27] Silva, R. F. and Zaniquelli, M.E.D. 2002. Morphology Of Nanometric Size Particulate Aluminium-Doped Zinc Oxide films. *Colloids and Surfaces A: Physicochemical and Engineering Aspects*. 198(200): 551-558.
- [28] Miller, F. A. and Wilkins, C. H. 1952. Infrared Spectra and Characteristic Frequencies of Inorganic Ions. *Analytical Chemistry*. 24(8): 1253-1294.
- [29] Palmer, S. J., Frost, R. L., Reddy, B. J. 2008. Characterisation Of Red Mud And Seawater Neutralised Red Mud Using Vibrational Spectroscopic Techniques. *8th International Alumina Quality Workshop*. 7(12).
- [30] Anedda, R., Cannas, C., Musinu, A., Pinna, G., Piccaluga, G. and Casu, M. 2008. A two-stage citric acid–sol/gel synthesis of ZnO/SiO₂ Nanocomposites: Study Of Precursors And Final Products. *J Nanopart Res*. 10(1): 107-120.
- [31] Oliveira, A. A. R. D., Gomide, V. S., Leite, M. D. F., Mansur, H. S., Pereira, M. D. M. 2009. Effect of Polyvinyl Alcohol Content and After Synthesis Neutralization on Structure, Mechanical Properties and Cytotoxicity of Sol-Gel Derived Hybrid Foams. *Materials Research*. 12(2): 239-244.
- [32] Brankovic, G., Brankovic, Z., Davolos, M.R., Cilense, M., Varela, J.A. 2004. Influence Of The Common Varistor Dopants (CoO, Cr₂O₃ and Nb₂O₅) On The Structural Properties Of SnO₂ Ceramics. *Materials Characterization*. 52(4-5): 243-251.